Accepted Manuscript

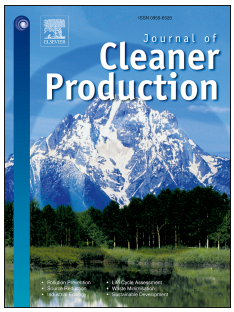

Simultaneous environmental and economic process synthesis of Isobutane Alkylation

Norberto García, María J. Fernández-Torres, José A. Caballero

PII: S0959-6526(14)00603-9

DOI: 10.1016/j.jclepro.2014.06.016

Reference: JCLP 4410

To appear in: *Journal of Cleaner Production*

Received Date: 19 November 2013

Revised Date: 3 June 2014

Accepted Date: 4 June 2014

Please cite this article as: García N, Fernández-Torres MJ, Caballero JA, Simultaneous environmental and economic process synthesis of Isobutane Alkylation, *Journal of Cleaner Production* (2014), doi: 10.1016/j.jclepro.2014.06.016.

Word count of our document, including the whole text file, including tables and figure captions = 7622

Simultaneous environmental and economic process synthesis of Isobutane Alkylation

Norberto García, María J. Fernández-Torres*, José A. Caballero

** Corresponding author: email fernandez@ua.es (Maria J. Fernández-Torres).*

Departamento de Ingeniería Química, University of Alicante, Apartado 99 E-03080 (Spain).

Tel: +34 965903400 (ext 2322); fax: +34 965903826.

ABSTRACT

This multidisciplinary study concerns the optimal design of processes with a view to both maximizing profit and minimizing environmental impacts. This can be achieved by a combination of traditional chemical process design methods, measurements of environmental impacts and advanced mathematical optimization techniques. More to the point, this paper presents a hybrid simulation-multiobjective optimization approach that at once optimizes the production cost and minimizes the associated environmental impacts of isobutane alkylation. This approach has also made it possible to obtain the flowsheet configurations and process variables that are needed to manufacture isooctane in a way that satisfies the above-stated double aim. The problem is formulated as a Generalized Disjunctive Programming problem and solved using state-of-the-art logic-based algorithms. It is shown, starting from existing alternatives for the process, that it is possible to systematically generate a superstructure that includes alternatives not previously considered. The optimal solution, in the form a Pareto curve, includes different structural alternatives from which the most suitable design can be selected. To evaluate the

environmental impact, Life Cycle Assessment based on two different indicators is employed: Ecoindicator 99 and Global Warming Potential.

Keywords:

Life Cycle Assessment; multiobjective optimization; Generalized Disjunctive Programming; Global Warming Potential; ecoindicator-99, isobutane alkylation.

1. Introduction

Over the last few decades there has been a clear shift toward an environmental awareness in many areas of society. What began as a social outcry is spreading to other areas such as the establishment of environmental regulations and inevitably to the research arena. In the field of process optimization, environmental factors were initially not taken into consideration and optimization was based only on profitability. Later, environmental considerations were introduced into the optimization problem by means of constraints. Finally, it is widely accepted that multiobjective (MO) optimization constitutes the best way to incorporate environmental criteria into the design of chemical processes if these are also to be profitable Azapagic (1999). As demonstrated in the previously cited study, the objective of "minimizing the environmental impact" can be comprehensively accounted for by means of Life Cycle Assessment (LCA) data (this, incidentally, is also the most widely accepted methodology nowadays). For instance, Morais et al. (2010) used LCA to compare three different process design alternatives by means of simulation for the production of biodiesel. The use of LCA in the design of sustainable chemical processes has two main advantages (Guillen-Gosalbez et al., 2007): In the first place, it covers the entire life of the product, process or activity and, in the second place, LCA aggregates the environmental burdens into a limited set of recognized environmental impact categories (depending on the LCA methodology used) such as Global Warming, acidification, ozone depletion, etc. For

that reason, LCA is a good framework to provide criteria and quantitative measures that can be used for comparing different process operation and design alternatives. The second objective, “maximizing profit”, is accounted for by means of the economic potential (EP) introduced in section 5.1 below.

The MO optimization methodology, which can accommodate both economic and environmental considerations, was first employed by Azapagic (1999) and has proved capable of providing the best set of design parameters that simultaneously addresses the economic and environmental problems. It has since then been applied in multiple case studies to be found in the literature. For instance, Jia et al. (2006) employed MO optimization in the context of cleaner production, and Erol and Thöming (2005) for the eco-design of reuse and recycling networks. Recent publications (Guillén-Gosálbez and Grossmann, 2010; Pozo et al., 2012; Ruiz-Femenia et al., 2013) employed it in the optimization of chemical supply chains. The subject of the study by García and Caballero (2011) was an economic and environmental assessment of various alternatives for extracting acetic acid from water. García and Caballero (2012) used the MO approach to study different options for a representative scheme of petrochemical processes characterized by raw feed materials containing impurities and inadequate single pass conversion in the reactor. Brunet et al. (2012) applied MO optimization to thermodynamic cycles. Torres et al. (2013) combined process simulation with environmental and economic performance evaluation for the optimization of a sour water stripping plant. Wang et al. (2013) obtained an optimal hydrocarbon biorefinery configuration (also from the viewpoint of sustainability) via gasification pathways using MO methodology. Gebreslassie et al. (2013a) followed a similar approach to attain the sustainable design and operation of a hydrocarbon biorefinery via fast pyrolysis, hydrotreating and hydrocracking. They consider such biorefineries to be promising industrial technologies based on their economic viability

and reduced greenhouse gas emissions. Gebreslassie et al. (2013b) devised the design and synthesis of an algae-based biorefinery that employs carbon sequestration, for the purpose of manufacturing a sustainable hydrocarbon-based biofuel. Shadiya et al. (2012) also employed MO optimization for the particular case of production of acrylonitrile, but they used the Waste Reduction Algorithm or WAR (Young and Cabezas, 1999) instead of LCA for the environmental impact assessment. Boix et al. (2012) studied industrial water management by MO optimization and found the best practical solution attending to both, environmental and economic criteria. Finally, we would like to include in this list, chapter 3 from the book written by Sharma and Rangaiah (2013) since these authors show the utility of MO optimization and illustrates it by means of multiple case studies.

The results of MO optimization are obtained in the form of a Pareto curve, which is a plot of an environmental impact variable against economic potential (see Fig.1). The Pareto curve in Fig.1 is a collection of the best set of alternatives that simultaneously meets both objectives (economic and environmental performance). An *inferior solution* (see Fig.1) occurs if there exits at least one better solution that can be attained without exacerbating the remaining objective functions. An *inferior solution* is also called a *dominated solution*. Therefore, a Pareto curve contains all the *non-inferior solutions* to the optimization problem (García and Caballero, 2011, 2012; Guillen-Gosalbez et al., 2007). This curve is also known as the *non-dominated alternatives*. In this paper, the set of *non-inferior solutions* has been obtained by means of the ε-constraint method (Ehrgott, 2005). Since each point on the Pareto curve represents a fixed process configuration that operates optimally, it is the job of the decision maker(s) to choose which of the trade-off solutions (or non-inferior solutions) on the curve meets their requirements.

The advantage of MO optimization over other methods that employ LCA methodology is that the generation of optimal solutions does not require establishing any type of subjective preferences beforehand to perform the optimization, since all potential solutions are evaluated (Azapagic, 1999). This implies that the importance of MO optimization is based more on the set of alternatives that can be chosen from the non-inferior solutions than on an explicit need to establish, at the outset of the optimization process, the priorities that are going to drive the synthesis of the chemical process without previously having considered all the trade-off solutions (Guillén-Gosálbez and Grossmann, 2010; Ruiz-Femenia et al., 2011).

2. Goal and scope definition

In this paper, the design and optimization of an isobutane alkylation process is treated as a multiobjective problem, which evaluates both environmental and economic functions at the same time. The process in question is the alkylation of light C4 olefins with isobutane to produce high octane components consisting of eight carbon atoms ("alkylate"). This is a very important process at many oil refineries. It is worth noting that the addition of an alkyl group to any compound is an alkylation reaction but in the context dealt with here, petroleum refining, the term alkylation is taken to mean the reaction of low molecular weight olefins with an isoparaffin to form higher molecular weight isoparaffins (Gary and Handwerk, 2001). Alkylation can take place at high temperatures in the absence of a catalyst. Nevertheless, industrial processes nowadays operate at moderate temperatures using either sulfuric or hydrofluoric acid as catalyst (Meyers, 2004). To carry out the MO optimization discussed in the present paper, sulfuric acid was used as catalyst.

The main objective of this work is to show how MO optimization combined with LCA and, particularly, with the EI-99 methodology and the GWP index is an effective procedure for

deciding which design and flow sheet are the best for the chemical process under consideration. There are different approaches for synthesizing a chemical process, however, the two most widely accepted alternatives are the conceptual design (Douglas, 1985, 1988; Smith, 2005) and the mathematical programming based approach (Grossmann et al., 1999; 2000). Although they were initially considered competitive, today process design involves contributions from both these approaches.

The synthesis of a process can be divided into three main steps (Grossmann et al., 1999):

1. Postulate a superstructure of alternatives (Yeomans and Grossmann, 1999). In the context of this paper, it is a schematic of all possible alternatives that represent the process under consideration.

2. Model the problem. Here, the problem is modeled as a Generalized Disjunctive Programming (GDP) problem, which allows it to be formulated as a discrete/continuous optimization problem (decision on the existence of a given configuration and its optimal operating conditions) using algebraic equations, disjunctions and logic propositions (Beaumont, 1990; Grossmann, 2002)

3. Solve the problem. GDP problems can be solved by reformulating them as mixed integer nonlinear programming (MINLP) (Grossmann, 2002), or using logic-based algorithms excluding the reformulation step (Lee and Grossmann, 2000, 2005; Türkay and Grossmann, 1996)

The rest of the paper is structured as follows: In section 3, a description is provided of the isobutane alkylation process together with some existing alternatives. Then, in section 4, based on that information, a superstructure of alternatives is proposed that include: (a) the existing ones, (b) an extension of the post reaction separation alternatives, (c) the possibility of feed purification as pretreatment, (d) purges, etc. Section 5 describes the

economic and environmental methodology, as well as the main hypothesis and assumptions made in each case. Section 6 contains comprehensive discussion of the results.

3. Isobutane alkylation processes

There are two commercial alkylation processes that utilize sulfuric acid as catalyst and that have been considered here for constructing the superstructure to be optimized, i.e., the base cases:

(a) The external refrigeration process (inspired by the process licensed by Stratford Engineering Corporation) and,

(b) The autorefrigeration process (licensed by Exxon Research and Engineering).

The information required about the process employing an externally refrigerated reactor (case (a) above) was obtained from Dimian and Bildea (2008). The initial configuration in the previously cited paper, which is summarized in Fig. 2, was used because it avoids the so-called "snowball effect". Dimian and Bildea (2008) assert that a plant with a recycle stream exhibits a snowball effect when it experiences a large nonlinear response in flows to small variations in certain parameters of the process units. Fig.2 shows two input streams to the process: a stream of pure isobutane (i-C4) and another containing 1-butene (C4) together with propane (C3). Propane behaves as an inert in this system. The kinetics and reaction data were also obtained from the above source. Advanced mechanisms to explain catalytic alkylation can be found in Dimian and Bildea (2008) and Gary and Handwerk (2001) among other sources, but the following simplified alkylation reaction schemes are widely accepted, and thus assumed here:

C4 + i-C4 → C8 (desired reaction)

C4 + C8 → C12 (unwanted reaction)

To avoid the unwanted reaction, an excess of i-C4 must be fed to the reactor. A sulfuric acid stream is also required as a catalyst for the reaction to take place. Because of the difference in density between the acid and hydrocarbon phases, a mixer is needed in the reactor chamber in order to obtain high product quality and yields. Since the intention is to use commercial simulators to perform the optimization, a CSTR has been chosen to achieve formation of a proper emulsion inside the reactor. After the reactor a liquid-liquid splitter will separate the acid from the remaining components, which require a posterior fractionation step. Direct separation was considered by Dimian and Bildea (2008): in the first column (C3-column), most of the inert (C3) is removed from the system; in the second column (C4-column), the reactants (C4 and i-C4) together with some C3 are separated from the products of the two reactions (C8 and C12) and recycled back to the reactor; in the third column (C8-column) the desired product (C8) is separated from the unwanted one (C12). The whole process operates at 8 bar of pressure, but the last separation column works at 1 bar. This configuration (see Fig. 2) is part of the basic starting flow sheet used to construct the superstructure handled in this paper.

Another potential configuration for the alkylation process superstructure is the autorefrigeration process presented by Luyben (2011) (case (b) above). A summary of this process configuration is shown in Fig. 3. It employs the same feed streams as Fig.2, which permits a proper comparison of the two processes shown in the two figures (the feed streams are slightly different in Luyben (2011). The olefin feed stream (C3 + C4) is split in three streams that feed each reactor. This second flow sheet differs from the first one (Fig.2) mainly because in the second, the reactors are auto-refrigerated by virtue of evaporation of a certain content from each reactor chamber. The most volatile components form a vapor phase. This vapor needs to be compressed to liquefy before it enters the C3

column. Here the inert leaves the process as overhead product. The bottoms of the C3 column, made up of C4 and i-C4, is recycled back to the reactors. The liquid phase leaving the third reactor enters a liquid-liquid splitter where the sulfuric acid is separated from the products of reaction. After removing the acid, the remaining liquid stream enters the C4 column where the C4 + i-C4 stream is separated as the overhead product. This stream joins the fresh i-C4 fed to the system along with the abovementioned C4 + i-C4 stream leaving the C3-column. The combined stream feeds the first reactor as shown in Fig.3. Finally, C8 and C12 are separated by means of another column (C8 column).

4. Superstructure and problem statement

In this section the superstructure to be optimized, that of the isobutane alkylation process using sulfuric acid as catalyst is described. It is shown in Fig.4, which is complemented by Fig.5. It has been assembled from a combination of the two options shown in Figs. 2 and 3 together with other potential alternatives. Different options were allowed in the superstructure for the optimization of the alkylation process, namely: (a) to separate hydrocarbons leaving the settling tank, all possible distillation sequences have been considered, from conventional ones to fully thermally coupled columns, going through all intermediate alternatives (e.g. direct and indirect splits, pre-fractionator, Petlyuk column arrangement, divided wall column, etc.) (Agrawal, 1996; Caballero and Grossmann, 2013; Shah and Agrawal, 2010) ;(b) to separate or not the propane (C3) from the olefin (C4) feed stream before it enters the system; (c) to split or not the stream leaving the settling tank so that propane can be distilled from a stream having a smaller molar flow rate; etc. Either 3 autorefrigerated reactors in series or just one externally refrigerated reactor were used in this superstructure, but the volume of the reaction mixture was allowed to vary.

Finally, the problem can be stated as follows. Find the flowsheet configuration and process variables – needed to manufacture isooctane – that simultaneously optimizes the production cost (maximizes EP) and minimizes the associated environmental impact. To that end, the superstructure shown in Fig. 4 has been considered. Fig. 5 completes Fig. 4 by revealing the separation superstructure scheme in detail.

5. Methodology

The MO optimization used here integrates environmental and economic assessment into the process design decisions to find the best process alternative that leads to an optimized design which is both "the greenest" and the most profitable. The approach taken was to couple the rigorous process simulation with the calculation and optimization of a set of environmental and economic indicators, as explained below.

5.1. Economic analysis

For the economic analysis, the economic potential (EP) as formulated in Smith (2005) was used since this criterion is preferred at the early stages of the design – it is particularly useful for comparing the relative advantages of different structural options in the flowsheet and different settings of the operating parameters. This term can be expressed as:

$$EP = value\ of\ products - annualized\ fixed\ costs - variable\ costs \quad (1)$$

The data used to estimate different equipment costs (fixed cost) were taken from Turton et al. (2003) and was updated using the Chemical Equipment Process Cost indexes (CEPCI).

To estimate the variable costs, the following features have been considered:

- Raw material costs: These costs are subject to an important degree of uncertainty: They can exhibit strong fluctuations due to market volatility and companies are reluctant to make this information public. Data used in this paper for isobutane and 1-butene are from Mahajanam et al. (2001). Table 1 shows the prices of these

substances as listed in the different sources, but data from different years are later updated in the optimization program to 2013.

- Selling price of reaction products: The selling price of isooctane was estimated from the breakeven (zero profit) value calculated in simulations. This value puts a lower limit on the selling price and the one used is a value higher than this. In any event, the real figure only shifts the Pareto curve sideways (Fig. 1), but does not affect the configuration found after the optimization, because different configurations at the same price and cost are compared. The selling price used in the simulation also appears in Table 1.

  It was decided that only isooctane is worth selling and that not much would be gained from selling propane or dodecane. This decision was taken to prevent the distortion of the calculation that results from the optimization process's attempt to produce more dodecane. It was instead elected to send these streams to a flare, and the environmental impact of this decision was also taken into account in performing the optimization.
- Utility operating costs: These constitute the most significant variable operating costs after raw materials. For an economic analysis of the superstructure, the costs of the electricity, cooling water, refrigerant and steam at different pressures were obtained from Turton et al. (2003).

To put fixed and variable costs on an equal footing, the capital cost has been expressed as total cost annualized (TCA) by assuming that it has been borrowed over a fixed period (5 years) at a fixed rate of interest (15%).

5.2. Environmental assessment

To assess the environmental impacts of the MO optimization, equations expressed in terms of indicators for the interactions between the process plant and the environment have been used. Two environmental impact methods have been selected to assess the superstructure in terms of environmental damage: a) Ecoindicator-99 (EI-99) and b) Global Warming Potential (GWP).

The interested reader is referred to the supplementary material A provided together with this manuscript for a brief description of these methods.

5.3. Simplifications and Main Hypothesis

To gauge the economic and environmental performance of the various possible flow sheets, a number of hypotheses have been made. They have been divided into two different categories: the economic evaluation (section 5.3.1) and the environmental assessment (section 5.3.2). Several simplifications are also possible in each case. Since these simplifications and hypotheses apply to all of the superstructure's potential configurations, they do not have an important effect on the final result (optimized flow sheet) – the relative merits of the various structural options or flow sheets are compared. Again, the difference will only shift the optimized Pareto curve (Fig. 1).

5.3.1. Economic Evaluation

The list of simplifications and main hypothesis on which the economic evaluation is based follow below:

• Only the expensive equipment is considered here and includes: CSTR, distillation columns, pumps, compressors, heaters, and coolers. The remaining equipment is expected to cost more or less the same for all potential flow sheets that can be derived from the superstructure, and its contribution to the fixed cost is assumed to be negligible.

• Estimates of the fixed and variable costs come from Turton et al. (2003).

• The following materials have been chosen to quantify the cost of the equipment:

- For the CSTR, stainless steel covered by Teflon was chosen due to the chemical incompatibility of stainless steel with sulfuric acid.
- For the heat exchangers, copper was chosen.
- For the compressors, carbon steel was chosen.
- For the centrifugal pumps, distillation columns, reboilers and condensers, carbon steel was selected.

• Column diameters were sized by means of the procedure described in a previous study (Towler and Sinnott, 2013)

• It is assumed that this industrial system operates under ideal conditions, and therefore there are no sulfuric acid losses or fugitive emissions from the chemical process. This statement also implies that no sulfuric acid or organic phase mixture is lost to the other phase, i.e., a complete separation of the two liquid phases is assumed to take place in the settling tank. This assumption was made even though in a real process the acid is diluted by unwanted reactions and feed contaminants, making it necessary to remove acid from the system and replenish it with a make-up stream of fresh sulfuric acid. The impact of this assumption is not very severe. For instance, isobutene is only slightly soluble in the acid phase, only to the extent of about 0.1 wt% in sulfuric acid. On the other hand, olefins are more soluble in the acid phase (Gary and Handwerk, 2001). In light of the above assumption, the reader might wonder why the superstructure includes a closed cycle of acid. The reason is the sulfuric acid concentration in the reactor must be high (Kirk et al., 2004). Therefore, the acid was only taken into account for calculating the reactor's true volume and for choosing the construction material because these factors affect its capital cost. The acid concentration was assumed to be 85 wt% in the reactor.

• As a further simplification, the simulations precluded the option, after the settler, of using a caustic wash to remove trace amounts of acid before sending the hydrocarbon stream to the distillation columns.

• The energy consumed by the CSTR stirrer was calculated by the method described in Sinnott et al. (1999).

• As discussed in section 5.1 and stated in Table 1, the C3, C12 and purge streams were sent to a flare (the possibility of commercializing these products was discarded). This was done based on the assumption that there was no profit to be made from them. As a consequence, their respective environmental impacts were taken into account when the two environmental methods considered here (EI-99 and GWP) were applied.

5.3.2. Environmental Evaluation

Below follows the list of simplifications and main hypothesis considered to carry out the environmental assessment:

• A functional unit (FU) of 7×10^5 t of pure C8 has been selected. This amount of C8 was estimated from a preliminary simulation where the mass flow rate of isooctane produced was multiplied by 30 years (operating time) with an estimated running time availability of 80%. Since each potential configuration of the proposed superstructure leads to a different production rate in the C8 stream, the plant operating time needed to reach the FU has been calculated for each of them.

• As stated in 4.3.1, no fugitive emissions due to catalyst and/or component losses to the environment are considered.

• The environmental impacts attributable to the materials of construction are not taken into consideration here because they are assumed to be more or less the same for all the different, yet similar flow sheet alternatives. Furthermore, these environmental impacts are

considered negligible compared with those that occur during the manufacture of the functional unit.

• Only two reactions are assumed to take place: a desirable reaction and a competing one, as described in section 3 above. So, apart from the reactants and products of these, it is assumed that there are no other substances present in the system.

• The environmental impacts of the raw materials used in the chemical process (directly proportional to the flow rates of the isobutane and 1-butane feed streams) have also been considered.

5.4 Mathematical model

The problem has been formulated as a hybrid simulation-optimization Generalized Disjunctive Programming (GDP) problem (Brunet et al., 2012; Caballero and Grossmann, 2010; Caballero et al., 2007) and was solved using a particular implementation of the logic-based outer approximation algorithm (Türkay and Grossmann, 1996). Aspen-HYSYS was used for all the thermodynamic properties calculation and all the equipment simulations apart from the distillation columns. For the distillation column simulations it was used the shortcut method by Underwood (1949), Fenske (1932), and Gilliland (1940), with the explicit equation by Molokanov et al. (1972) and Kirkbride (1944) for the feed tray location implemented in Matlab ™ and connected to Aspen-HYSYS through the activeX capabilities (in any case, the final results were checked with a rigorous model). Physical properties (e.g. relative volatilities estimation) and condensers and reboilers were rigorously calculated using Aspen-HYSYS. For the simulation of thermal couples the approach described in Navarro-Amorós et al. (2013) was followed. The details of the calculation of the sequence of distillation columns are too extensive to be included here but a comprehensive description can be found in the following references (Caballero and Grossmann, 2001, 2006, 2013). However, we would at least like to remark that all the alternatives from

conventional to fully thermally coupled configurations (including divided wall columns) have been included. The interested reader is referred to the supplementary material B for a detailed description of the mathematical model that underpins all the calculations that have been performed.

6. Results and discussion

This section describes the results of the application of multiobjective optimization to the superstructure presented in Fig. 4 and complemented by Fig. 5. It is important to emphasize that the environmental results presented here are a true reflection of the environmental impacts that can be attributed to the functional unit, taking into account the simplifications previously explained in section 5.3.2. Although there are some inaccuracies in the assumed cost of raw materials and selling price of the product, the obtained results are useful because they allow the user to compare different configurations with each other. Even though there is bound to be some degree of error in the final numerical result calculated from the economic potential and the environmental parameters used, the final optimized structures (flow diagrams together with operational parameters) are the best choice. The optimization process led to the two optimized Pareto curves shown in Fig. 6: one pertaining to the case in which the EI-99 environmental indicator was minimized and the other, when it was the GWP. In both cases, the X-axis indicates the Economic Potential (EP). A couple of '*stars'* has been used to mark the environmental and the economic optima on the GWP and EI-99 Pareto curves (Fig. 6) , i.e., the two extremes or p-anchor points of both Pareto curves. They have also been labeled with an A and a B for reference in the subsequent discussion. For purposes of comparison, Fig. 6 also contains the Pareto curve corresponding to the flowsheet diagram with external refrigeration, adapted from the initial configuration in Dimian and Bildea (2008). This configuration avoids the so called

"snowball effect" – using GWP as environmental indicator – and was also considered as a potential configuration in the proposed superstructure (see Fig. 2). It is worth noting that the above mentioned configuration results in an inferior solution or one that is dominated by the other optimal ones found in this work.

Table 2 lists information about the extreme points on the two Pareto curves. In the case involving the GWP indicator, the breakeven selling price of isooctane has been calculated by setting the value of EP equal to zero (no profit) in Eq. (1) and using the information provided in Tables 3 and 4. The isooctane breakeven selling price calculated in this way was 0.42 $/kg for the economic optimum and 0.86 $/kg for environmental optimum. This parameter should be taken into account because the isooctane market price can influence decision makers about the most appropriate configuration in terms of competitiveness with other suppliers of isooctane.

The Pareto curves shown in Fig.6, one obtained by minimizing EI-99 and the other GWP (both maximize EP), exhibit similar shapes even though they are plotted in different units (eco-indicator points/functional unit and kg CO_2 eq/functional unit, respectively). This similitude in shape can be attributed to the fact that the main environmental impacts of the superstructure occur in the form of energy consumption (especially electricity and heat energy requirements), which both environmental indicators properly take into account.

The MO optimization results (the two Pareto curves) are compounded by three configurations and labeled as "1st Solution", "2nd Solution" and "3rd Solution" in Fig. 6. So, there is not a single optimal configuration in the superstructure that converges to the best results and that also meets both criteria (maximizing EP while simultaneously minimizing any of the two environmental indicators: EI-99 or GWP). These composite Pareto curves

represent the best configurations for carrying out the isobutane alkylation. Each solution, or configuration, is presented and described briefly in Fig. 7. Fig.6 demonstrates that the 1st solution, see Table 4 for the corresponding operating conditions, is accompanied by the lowest environmental impacts (with respect to both environmental indicators; EI-99 and GWP). However, its economic potential is also the worst in comparison with the 2nd and 3rd solutions or configurations. On the other hand, the auto-refrigerated alternative (3rd solution, see Fig.3 and Table 3) is the best solution based only on the economic criterion, but involves the highest environmental impact near its right end. At this point, it will be up to the decision maker to assess these results and to decide which configuration (and corresponding optimal operating conditions) to use in the end.

From Fig. 6 it can be seen that the 3rd solution is clearly the "best" and most suitable configuration for carrying out the isobutane alkylation. The steep slope of the curve near its right end implies the possibility of using a configuration accompanied by substantially less environmental damage without affecting the value of the economic potential too much. For instance, if decided to operate under conditions at which the EP does not equal its maximum value, 38.2 $MM/y on the GWP curve and 39.2 $MM/y on the EI-99, but 37.5 $MM/y - (a slight drop of 1.8% and 4.3% along the GWP and EI-99 curves, respectively) the environmental indicators serving as proxies for environmental damage would drop substantially (a 21.5% and 24.9% drop in GWP and EI-99, respectively). In any case, it is important to point out that choosing the best configuration (and its operating conditions) from a Pareto curve is always a subjective decision since all solutions are equivalent from a mathematical point of view. The identification of non-inferior solutions provides a valuable insight into the design problem, however, and is intended to guide the decision maker in choosing a more sustainable process alternative leading to the best profit at a fixed environmental impact, or vice versa.

The functions EP, GWP and EI-99 are evaluated at every iteration during the optimization process. The optimization is accomplished by maximizing EP and minimizing either one of the two environmental indicators selected beforehand. But even though the optimization was conducted by selecting only one of the two environmental indicators at a time, the readings for the other environmental indicator were also included in the final results. Hence, the optimized solution consists of one EP value and the optimized value of the preselected environmental indicator, and also includes a reading for the other environmental indicator under the optimized conditions. The total amount of information captured during the optimization process is considerable when this approach is taken. In addition, a breakdown of all of the environmental burdens was calculated and recorded. All this information, which enhances interpretation of the results, is presented as a collection of charts in the supplementary material C given.

As pointed out earlier, Tables 3 and 4 contain details of the configurations corresponding to the two extremes on the Pareto curve that are optimal with respect to GWP (Points A and B on the GWP curve in Fig. 6), i.e., Table 3 shows the parameters of the best solution when the optimization function maximizes the economic potential, whereas Table 4 presents the parameters of the best solution when the optimization function minimizes the environmental impact. Both tables contain relevant data such as, for instance, the molar flow rate of isooctane produced (plant capacity) and the molar flow rates of propane and dodecane that have been sent to a flare.

Finally, Fig. 8 shows, using figures that have been normalized to 1, the difference between the two extremes on the Pareto curve (economic and environmental optima on the GWP

curve) in terms of the 12 impact sub-categories of the Ecoindicator model. There it can be clearly seen that the highest environmental impact falls under the “fossil fuel” subcategory.

7. Conclusions

A cleaner industrial process for producing alkylate has been designed that at same time minimizes the environmental impact and maximizes the economic profit of the process. This trans-disciplinary research effort was tackled by means of a hybrid simulation-multiobjective optimization approach. In particular, the process’s environmental impact was minimized through Life Cycle Assessment (LCA), which leads to performance that is both improved and environmentally holistic.

By following the above procedure the design of new and optimal production strategies have been accomplished. Three different structural alternatives were generated in this way. They are by design more sustainable than those obtained by other commercial strategies, because they are accompanied by lower energy consumption and cleaner production. Justifications for selecting one of the three optimal structures over the other two have also been provided.

The optimization process presented here can, on the one hand, show how to accelerate the adoption of cleaner production by industries. On the other, it also represents an example of a comprehensive solved problem that can be used as educational material to illustrate the manner in which optimization tools can aid the sustainable design of industrial processes.

Acknowledgements

We acknowledge the support from the Spanish Ministry of Science and Innovation (CTQ2012-37039-C02-02) and to Mr. W. Dednam for proofreading the article.

References

Agrawal, R., 1996. Synthesis of Distillation Column Configurations for a Multicomponent Separation. Ind. Eng. Chem. Res. 35, 1059-1071.
Azapagic, A., 1999. Life cycle assessment and its application to process selection, design and optimisation. Chem. Eng. J. 73, 1-21.
Beaumont, N., 1990. An algorithm for disjunctive programs. Eur. J. Oper. Res. 48, 362-371.
Boix, M., Montastruc, L., Pibouleau, L., Azzaro-Pantel, C., Domenech, S., 2012. Industrial water management by multiobjective optimization: from individual to collective solution through eco-industrial parks. J. Clean. Prod. 22, 85-97.
Brunet, R., Cortés, D., Guillén-Gosálbez, G., Jiménez, L., Boer, D., 2012. Minimization of the LCA impact of thermodynamic cycles using a combined simulation-optimization approach. Appl. Therm. Eng. 48, 367-377.
Caballero, J.A., Grossmann, I.E., 2001. Generalized Disjunctive Programming Model for the Optimal Synthesis of Thermally Linked Distillation Columns. Ind. Eng. Chem. Res. 40, 2260-2274.
Caballero, J.A., Grossmann, I.E., 2006. Structural Considerations and Modeling in the Synthesis of Heat-Integrated−Thermally Coupled Distillation Sequences. Ind. Eng. Chem. Res. 45, 8454-8474.
Caballero, J.A., Grossmann, I.E., 2010. Hybrid Simulation-Optimization Algorithms for Distillation Design, in: Pierucci, S., Ferraris, G.B. (Eds.), Computer Aided Chemical Engineering. Elsevier, pp. 637-642.
Caballero, J.A., Grossmann, I.E., 2013. Synthesis of complex thermally coupled distillation systems including divided wall columns. AIChE J. 59, 1139-1159.
Caballero, J.A., Odjo, A., Grossmann, I.E., 2007. Flowsheet optimization with complex cost and size functions using process simulators. AIChE J. 53, 2351-2366.
Dimian, A.C., Bildea, C.S., 2008. Chemical process design : computer-aided case studies. Wiley-VCH, Weinheim Chichester.
Douglas, J.M., 1985. A hierarchical decision procedure for process synthesis. AIChE J. 31, 353-362.
Douglas, J.M., 1988. Conceptual Design of Chemical Processes. McGraw-Hill., New York.
Ehrgott, M., 2005. Multicriteria optimization, 2nd ed. Springer, Berlin ; New York.
Erol, P., Thöming, J., 2005. ECO-design of reuse and recycling networks by multi-objective optimization. J. Clean. Prod. 13, 1492-1503.
Fenske, M.R., 1932. Fractionation of Straight-Run Pennsylvania Gasoline. Ind. Eng. Chem. 24, 482-485.
García, N., Caballero, J.A., 2011. Economic and Environmental Assessment of Alternatives to the Extraction of Acetic Acid from Water. Ind. Eng. Chem. Res. 50, 10717-10729.
García, N., Caballero, J.A., 2012. How to implement environmental considerations in chemical process design: An approach to multiobjective optimization for undergraduate students. Educ. Chem. Eng. 7, e56-e67.
Gary, J.H., Handwerk, G.E., 2001. Petroleum refining : technology and economics, 4th ed. Marcel Dekker, New York.
Gebreslassie, B.H., Slivinsky, M., Wang, B., You, F., 2013a. Life cycle optimization for sustainable design and operations of hydrocarbon biorefinery via fast pyrolysis, hydrotreating and hydrocracking. Comput. Chem. Eng. 50, 71-91.
Gebreslassie, B.H., Waymire, R., You, F., 2013b. Sustainable design and synthesis of algae-based biorefinery for simultaneous hydrocarbon biofuel production and carbon sequestration. AIChE J. 59, 1599-1621.
Gilliland, E.R., 1940. Multicomponent Rectification Estimation of the Number of Theoretical Plates as a Function of the Reflux Ratio. Ind. Eng. Chem. 32, 1220-1223.

Grossmann, I.E., 2002. Review of Nonlinear Mixed-Integer and Disjunctive Programming Techniques. Optim. Eng. 3, 227-252.
Grossmann, I.E., Caballero, J.A., Yeomans, H., 1999. Mathematical programming approaches to the synthesis of chemical process systems el mío. Korean J. Chem. Eng. 16, 407-426.
Grossmann, I.E., Caballero, J.A., Yeomans, H., 2000. Advances in mathematical programming for the synthesis of process systems. Latin Am. Appl. Res. 30, 263-284.
Guillen-Gosalbez, G., Caballero, J.A., Jimenez Esteller, L., Gadalla, M., 2007. Application of life cycle assessment to the structural optimization of process flowsheets, in: Plesu, V., Agachi, P.S. (Eds.), pp. 1163-1168.
Guillén-Gosálbez, G., Grossmann, I., 2010. A global optimization strategy for the environmentally conscious design of chemical supply chains under uncertainty in the damage assessment model. Comput. Chem. Eng. 34, 42-58.
Jia, X., Zhang, T., Wang, F., Han, F., 2006. Multi-objective modeling and optimization for cleaner production processes. J. Clean. Prod. 14, 146-151.
Kirk, R.E., Othmer, D.F., Kroschwitz, J.I., Seidel, A., 2004. Kirk-Othmer encyclopedia of chemical technology, 5th ed. Wiley-Interscience, Hoboken, NJ.
Kirkbride, C.G., 1944. Process Design Procedure for Multicomponent Fractionators. . Petroleum Refiner. 23, 321-336.
Lee, S., Grossmann, I.E., 2000. New algorithms for nonlinear generalized disjunctive programming. Comput. Chem. Eng. 24, 2125-2141.
Lee, S., Grossmann, I.E., 2005. Logic-Based Modeling and Solution of Nonlinear Discrete/Continuous Optimization Problems. Ann Oper Res 139, 267-288.
Luyben, W.L., 2011. Principles and case studies of simultaneous design. John Wiley & sons, Hoboken, N.J., p. 324 p.
Mahajanam, R.V., Zheng, A., Douglas, J.M., 2001. A shortcut method for controlled variable selection and its application to the butane alkylation process. Industrial and Engineering Chemistry Research 40, 3208-3216.
Meyers, R.A., 2004. Handbook of petroleum refining processes, 3rd ed. McGraw-Hill, New York.
Molokanov, Y.K., Korablina, T.P., Mazurina, N.I., Nikiforov, G.A., 1972. An Approximation Method for Calculating the Basic Parameters of Multicomponent Fraction. Int. Chem. Eng. 12, 209.
Morais, S., Mata, T.M., Martins, A.A., Pinto, G.A., Costa, C.A.V., 2010. Simulation and life cycle assessment of process design alternatives for biodiesel production from waste vegetable oils. J. Clean. Prod. 18, 1251-1259.
Navarro-Amorós, M.A., Caballero, J.A., Ruiz-Femenia, R., Grossmann, I.E., 2013. An alternative disjunctive optimization model for heat integration with variable temperatures. Comput. Chem. Eng. 56, 12-26.
Pozo, C., Ruiz-Femenia, R., Caballero, J., Guillén-Gosálbez, G., Jiménez, L., 2012. On the use of Principal Component Analysis for reducing the number of environmental objectives in multi-objective optimization: Application to the design of chemical supply chains. Chem. Eng. Sci. 69, 146-158.
Ruiz-Femenia, R., Caballero, J.A., Jiménez, L., 2011. Minimization of the life cycle impact of chemical supply chain networks under demand uncertainty, pp. 1195-1199.
Ruiz-Femenia, R., Guillén-Gosálbez, G., Jiménez, L., Caballero, J.A., 2013. Multi-objective optimization of environmentally conscious chemical supply chains under demand uncertainty. Chem. Eng. Sci. 95, 1-11.
Shadiya, O.O., Satish, V., High, K.A., 2012. Process enhancement through waste minimization and multiobjective optimization. J. Clean. Prod. 31, 137-149.
Shah, V.H., Agrawal, R., 2010. A matrix method for multicomponent distillation sequences. AIChE J. 56, 1759-1775.

Sharma, S., Rangaiah, G.P., 2013. Chapter 3: Multi-Objective Optimization Applications in Chemical Engineering, Multi-Objective Optimization in Chemical Engineering. John Wiley & Sons Ltd, pp. 35-102.
Sinnott, R.K., Coulson, J.M., Richardson, J.F., 1999. Chemical engineering. Vol. 6, Chemical engineering design, 3rd ed. Butterworth-Heinemann, Oxford.
Smith, R., 2005. Chemical process design and integration. Wiley, Chichester ; Hoboken, NJ.
Torres, C.M., Gadalla, M., Mateo-Sanz, J.M., Jiménez, L., 2013. An automated environmental and economic evaluation methodology for the optimization of a sour water stripping plant. J. Clean. Prod. 44, 56-68.
Towler, G.P., Sinnott, R.K., 2013. Chemical engineering design : principles, practice, and economics of plant and process design, 2nd ed. Butterworth-Heinemann, Oxford ; Waltham, MA.
Türkay, M., Grossmann, I.E., 1996. Logic-based MINLP algorithms for the optimal synthesis of process networks. Comput. Chem. Eng. 20, 959-978.
Turton, R., Bailie, R.C., Whiting, W.B., Shaeiwitz, J.A., 2003. Analysis, synthesis, and design of chemical processes, 2nd ed. Prentice Hall/PTR, Upper Saddle River, N.J.
Underwood, A.J.V., 1949. Fractional Distillation of Multicomponent Mixtures. Ind. Eng. Chem. 41, 2844-2847.
Wang, B., Gebreslassie, B.H., You, F., 2013. Sustainable design and synthesis of hydrocarbon biorefinery via gasification pathway: Integrated life cycle assessment and technoeconomic analysis with multiobjective superstructure optimization. Comput. Chem. Eng. 52, 55-76.
Yeomans, H., Grossmann, I.E., 1999. A systematic modeling framework of superstructure optimization in process synthesis. Comput. Chem. Eng. 23, 709-731.
Young, D.M., Cabezas, H., 1999. Designing sustainable processes with simulation: the waste reduction (WAR) algorithm. Comput. Chem. Eng. 23, 1477-1491.

TABLES:

Table 1

Costs and selling prices used in our research (data from different years are later updated in the optimization program to 2013).

		Source
Raw material costs	• isobutane: 0.70 $/kg • 1-butene: 0.46 $/kg	(Mahajanam et al., 2001)
Products selling price	• Isooctane: 1.9 $/kg • Propane: N/A • Dodecane: N/A	A higher value than the breakeven (section 6).
Utility operation costs	• Refrigeration at – 20ºC: 7.89 $/GJ • Refrigeration at 15ºC: 4.43 $/GJ • Electricity: 16.8 $/GJ • Process steam (low pressure): 6.08 $/GJ • Process steam (medium pressure): 6.87 $/GJ • Process steam (high pressure): 9.83 $/GJ • Process cooling water: 0.354 $/GJ	(Turton et al., 2003)

Table 2

Information about the p-anchor points shown in Fig. 6.

	Maximizing Economic Potential (EP)			
	Minimizing Ecoindicator-99		**Minimizing GWP**	
	Economic optimum	**Environmental optimum**	**Economic optimum**	**Environmental optimum**
EP (Economic Potential), eq. (1) for a selling price of C8 of \$1.9/kg	\$39.2 MM/y	\$15.5 MM/y	\$38.2 MM/y	\$15.5 MM/y
Environmental indicator	2.5×10^9 Points/FU	0.8×10^9 Points/FU	31.0×10^9 kg CO_2 eq/FU	10.6×10^9 kg CO_2 eq /FU

Table 3

Details of the configuration of the superstructure which drives to the maximum Economic Potential – 3rd solution in Figure 6 (GWP curve – Point A) and Fig.7.

Main equipment characteristics:

Reactor (1, 2 or 3):

Volume = 13.89 m^3

Heat flow = 0 kW

C3 column:

Number of trays: 8 (rectifying) 24 (stripping)

Reboiler heat: 1348.4 kW

Condenser heat: 1032.3 kW

Distillate temperature =48.3 ºC

Bottoms temperature = 85.5 ºC

Compressor 1 (K1):

Shaft work = 14.5 kW

Compressor 1 (K2):

Shaft work = 11.3 kW

Compressor 1 (K3):

Shaft work = 166.1 kW

Heat exchanger 1 (HX1):

Heat flow = - 785.2 kW

Heat exchanger 1 (HX2):

Heat flow = -2666.7 kW

C4 Column:

Number of trays: 9(r) and 5(s)

Reboiler heat= 10373.1 kW

Condenser heat= 4935.8 kW

Distillate temperature =47.4 ºC

Bottoms temperature = 182.7 ºC

Lights pump:

Shaft work = 5.6 kW

Heavies pump:

Shaft work = 18.5 kW

C8 column:

Number of trays: 11(r) and 4(s)

Reboiler heat= 64.1 kW

Condenser heat= 202.1 kW

Distillate temperature =95.6 ºC

Bottoms temperature = 165.5 ºC

Total molar flow rates & molar fractions of selected streams:

- C3+C4 feed stream:
  - Flow rate= 40.0 kmol/h
  - x_{C4} = 0.7854
- i-C4 feed stream:
  - Flow rate= 31.2 kmol/h
  - $x_{i\text{-}C4}$ = 1
- C8 product stream
  - Flow rate = 28.5 kmol/h
  - x_{C8} =0.9915
- C12 product stream
  - Flow rate = 1.6 kmol/h
  - x_{C12} =0.8214
- C3 product stream
  - Flow rate = 10.0 kmol/h
  - x_{C3} =0.8611
- recycle stream (@ -1.6 ºC)
  - Flow rate = 1123.1 kmol/h
  - $x_{i\text{-}C4}$ =0.9583

Table 4

Details of the configuration of the superstructure which drives to the minimum Global Warming Potential – 1st solution in Figure 6 (GWP curve – Point B) and Fig.7.

Main equipment characteristics:

C3+C4 compressor:

Shaft work = 78.0 kW

i-C4 compressor:

Shaft work = 45.6 kW

Reactor:

Volume = 87.19 m^3

Heat flow = -1475.2 kW

C8 column:

Number of trays: 5 (rectifying) 4 (stripping)

Reboiler heat: 22.5 kW

Condenser heat: 173.9 kW

Distillate temperature =100.0 ºC

Bottoms temperature = 207.7 ºC

Heat exchanger:

Heat flow = +404.6 kW

Divided Wall Column:

Number of trays in each section:

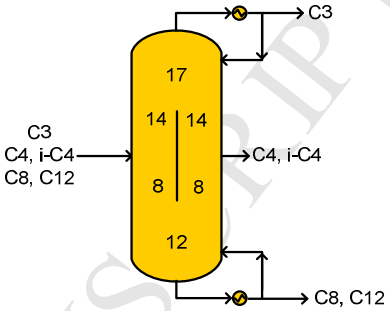

Reboiler heat= 1493.7 kW

Condenser heat= 533.2 kW

Distillate temperature =16.9 ºC

Bottoms temperature = 215.6 ºC

Recycle pump:

Shaft work = 0.2 kW

Total molar flow rates & molar fractions of selected streams:

- C3+C4 feed stream:
  Flow rate= 40.0 kmol/h
  x_{C4} = 0.7854
- i-C4 feed stream:
  Flow rate= 24.0 kmol/h
  $x_{i\text{-}C4}$ = 1
- C8 product stream
  Flow rate = 16.4 kmol/h
  x_{C8} =0.9953
- C12 product stream
  Flow rate = 7.6 kmol/h
  x_{C12} =0.9783
- C3 product stream
  Flow rate = 8.6 kmol/h
  x_{C3} =0.9943
- recycle stream (@ 55.0ºC)
  Flow rate = 107.3 kmol/h
  $x_{i\text{-}C4}$ =0.9703

Usable black and white prints corresponding to all the color illustrations

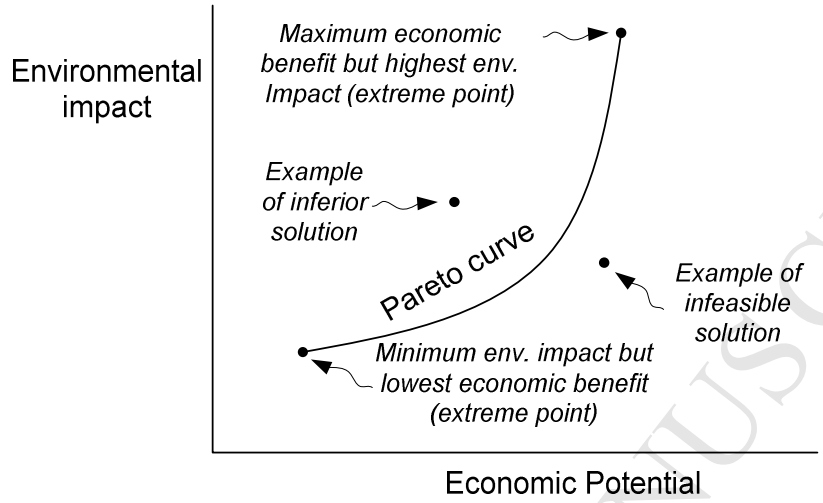

Fig.1. *Schematic of the Pareto curve obtainable by the multiobjective (MO) optimization method*

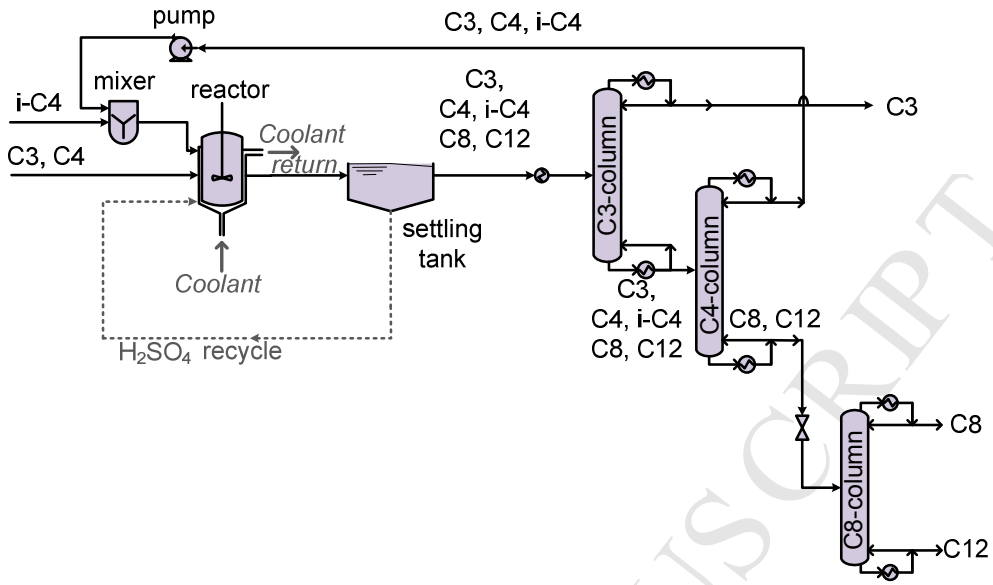

Fig. 2. *Flowsheet diagram with external refrigeration taken from the initial configuration in Dimian and Bildea (2008) that avoids the so called "snowball effect".*

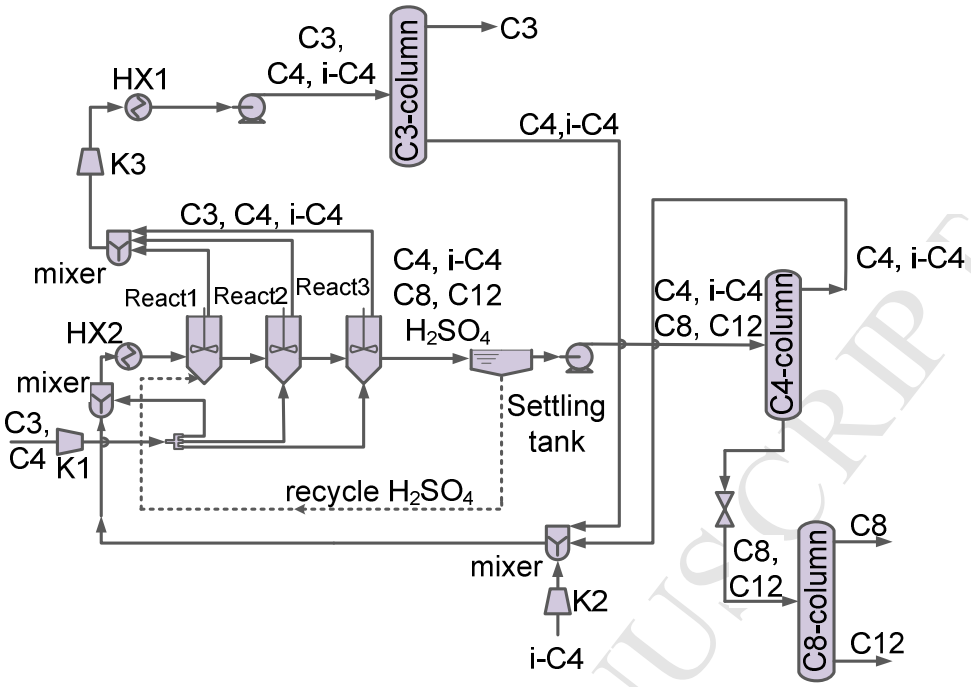

Fig. 3. *Flowsheet diagram with auto-refrigerated reactors based on Luyben (2011). K_i and HX_i refer to compressors and heat exchanger respectively.*

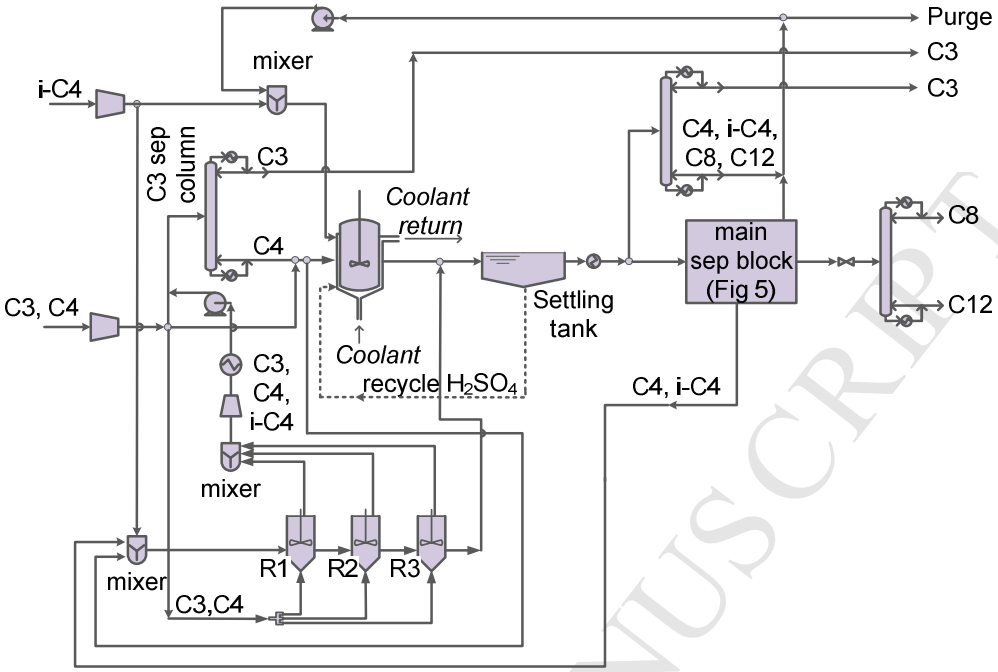

Fig. 4. *Superstructure for the synthesis of isooctane (C8). The details of the main separation block, represented here by a box, are shown in Fig. 5. R_i refer to the reactors*

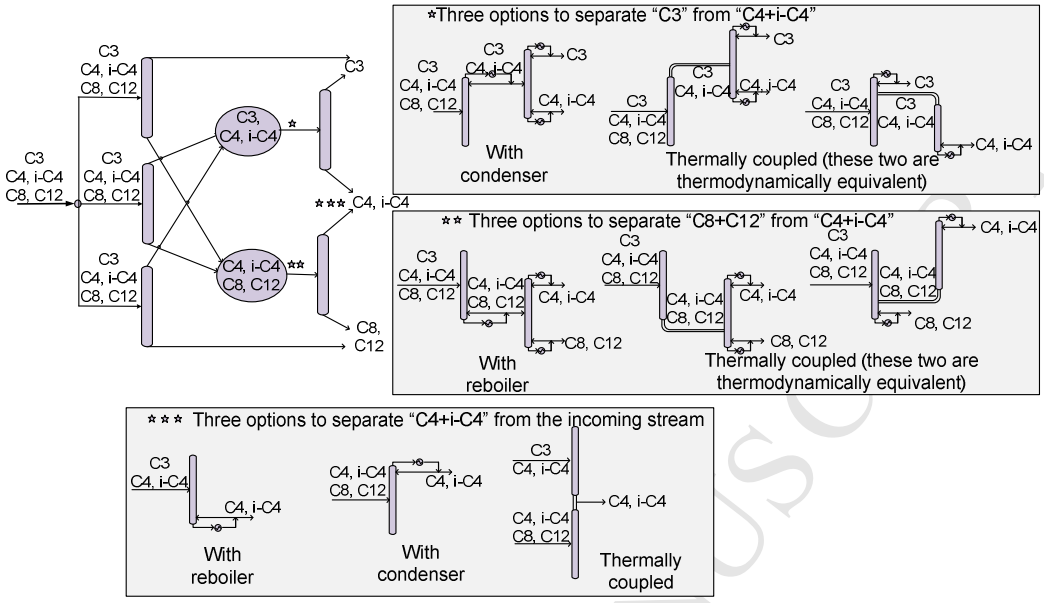

Fig. 5. *Main separation block: Separation superstructure scheme corresponding to Fig. 4.*

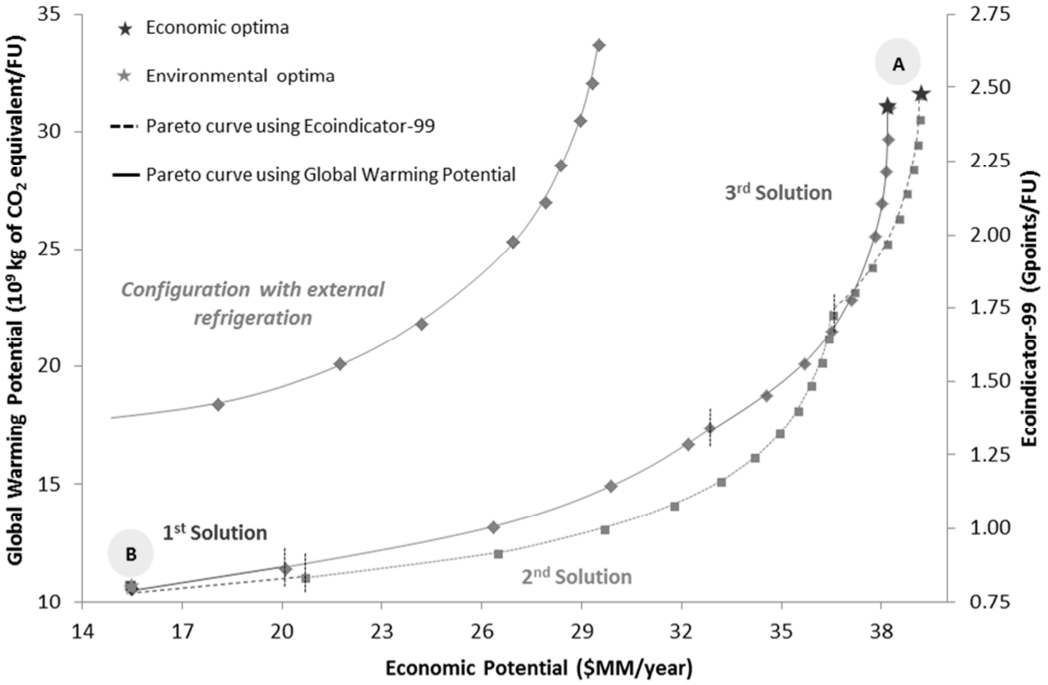

Fig 6. *Pareto curves for both environmental indicators (EI-99 and GWP). The configuration with external refrigeration (see Fig.2) is shown for comparison. See the details of the three solutions in Fig. 7.*

1st Solution: Configuration where the main separation is achieved with a divided wall column.

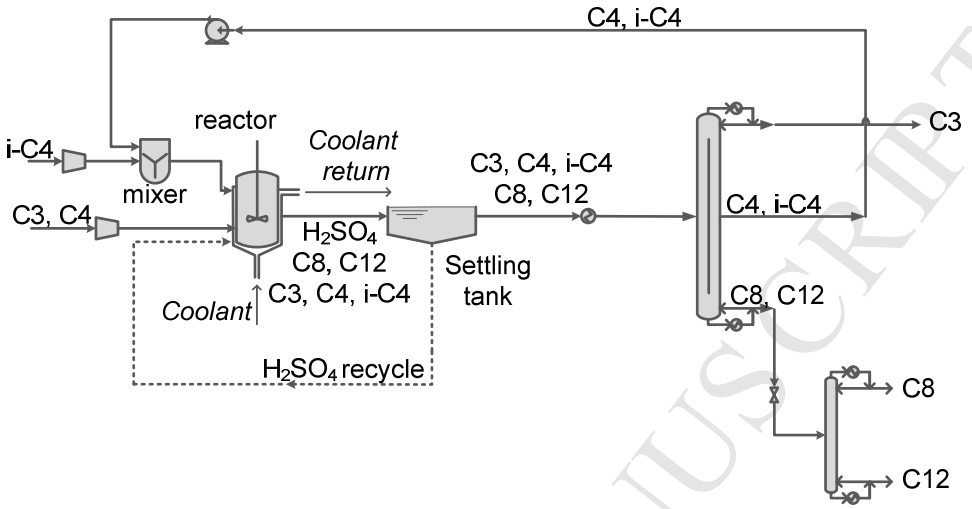

2nd Solution: Configuration where the separation uses a prefractionator without thermal couple

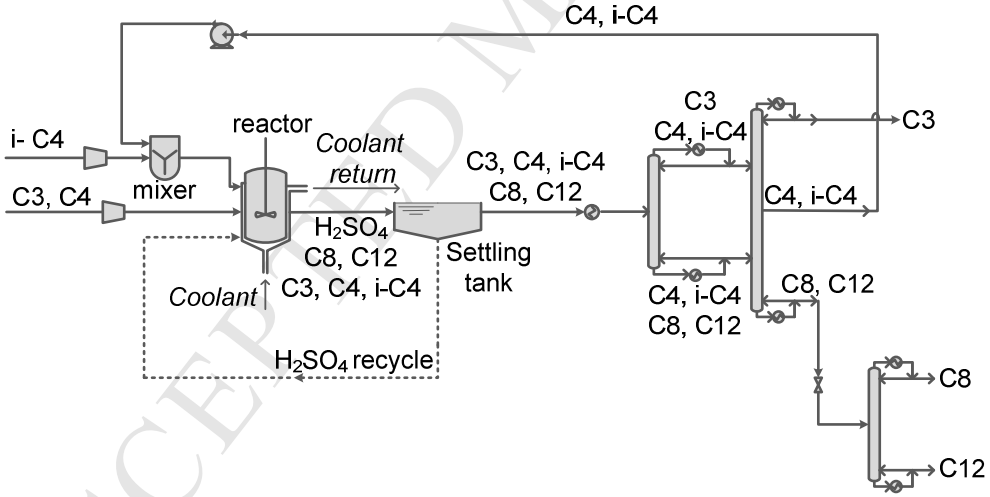

3rd Solution: See Fig.3. Configuration where the reaction takes place in three auto-refrigerated reactors in series.

Fig 7. *Configurations that fall on the Pareto curve (set of non-inferior solutions) in Fig. 6.*

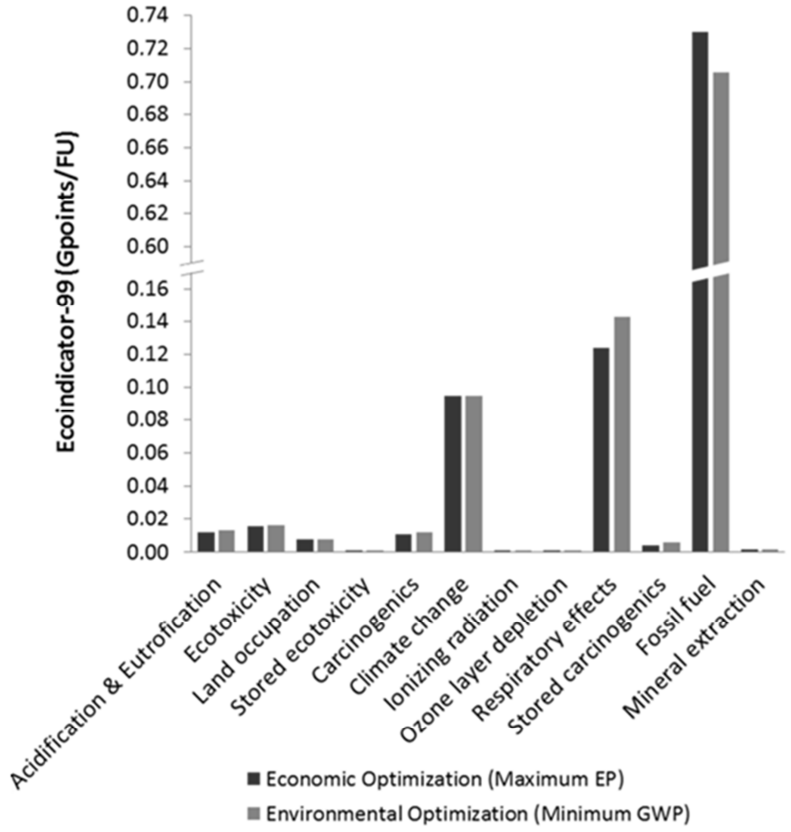

Fig. 8. *Normalized environmental subcategories of the EI-99 Pareto curve shown in Fig.6*

Table 4

Details of the configuration of the superstructure which drives to the minimum Global Warming Potential – 1st solution in Figure 6 (GWP curve – Point B) and Fig.7.

Main equipment characteristics:

C3+C4 compressor:

Shaft work = 78.0 kW

i-C4 compressor:

Shaft work = 45.6 kW

Reactor:

Volume = 87.19 m^3

Heat flow = -1475.2 kW

C8 column:

Number of trays: 5 (rectifying) 4 (stripping)

Reboiler heat: 22.5 kW

Condenser heat: 173.9 kW

Distillate temperature =100.0 ºC

Bottoms temperature = 207.7 ºC

Heat exchanger:

Heat flow = +404.6 kW

Divided Wall Column:

Number of trays in each section:

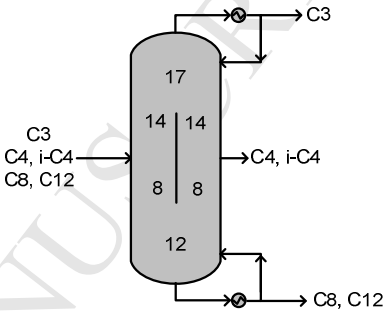

Reboiler heat= 1493.7 kW

Condenser heat= 533.2 kW

Distillate temperature =16.9 ºC

Bottoms temperature = 215.6 ºC

Recycle pump:

Shaft work = 0.2 kW

Total molar flow rates & molar fractions of selected streams:

- C3+C4 feed stream:
  - Flow rate= 40.0 kmol/h
  - x_{C4} = 0.7854
- i-C4 feed stream:
  - Flow rate= 24.0 kmol/h
  - $x_{i\text{-}C4}$ = 1
- C8 product stream
  - Flow rate = 16.4 kmol/h
  - x_{C8} =0.9953
- C12 product stream
  - Flow rate = 7.6 kmol/h
  - x_{C12} =0.9783
- C3 product stream
  - Flow rate = 8.6 kmol/h
  - x_{C3} =0.9943
- recycle stream (@ 55.0ºC)
  - Flow rate = 107.3 kmol/h
  - $x_{i\text{-}C4}$ =0.9703

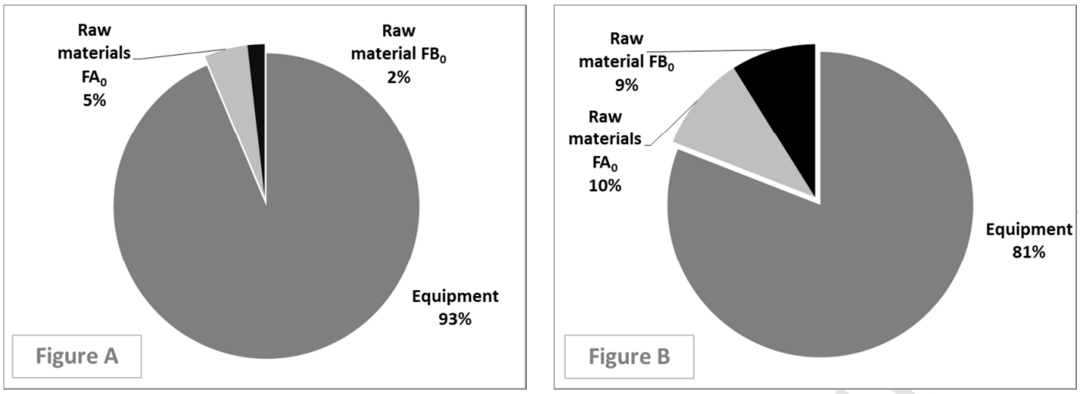

Fig. C.1. *Breakdown of the environmental impacts at optimum economic potential when the system is optimized using GWP as the environmental indicator. FA_o stands for the feed stream containing C3 and C4, shown in the superstructure (Fig.4). FB_o stands for the feed stream containing i-C4*

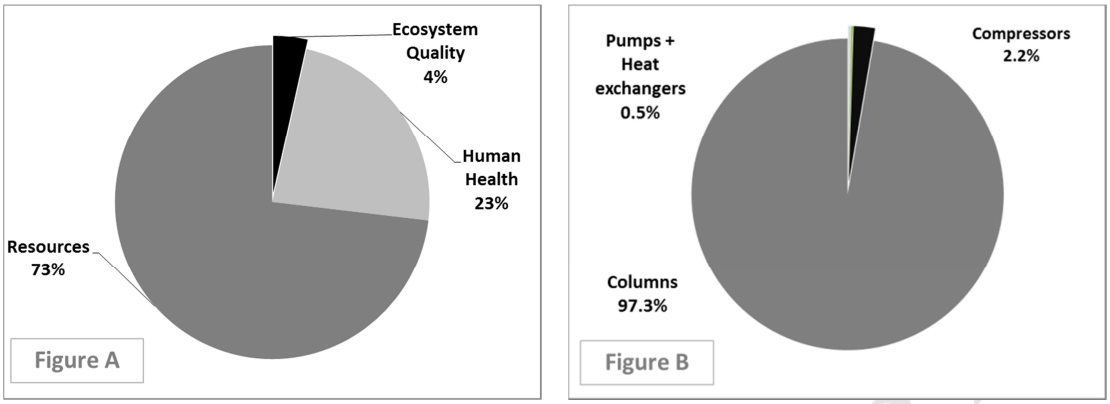

Fig C.2. *Breakdown of the environmental burdens at optimum economic potential according to Ecoindicator-99, when the superstructure is optimized using EP and GWP (Point A on the GWP Pareto curve in Fig. 6).*

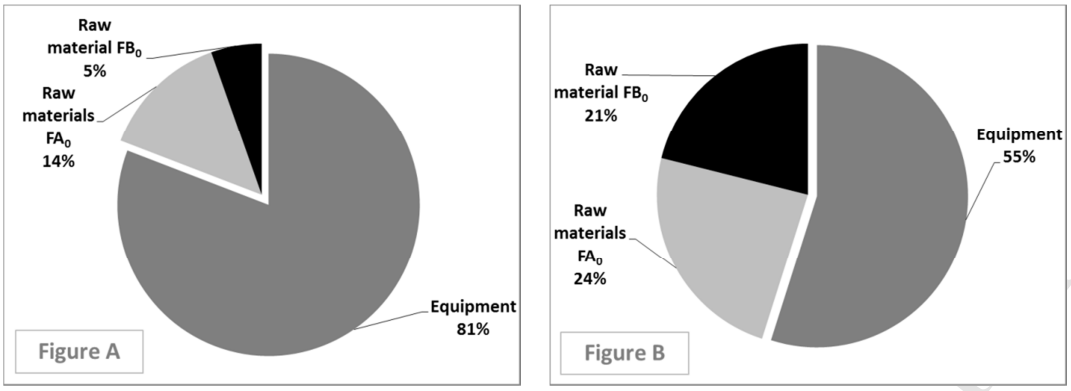

Fig. C.3. *Breakdown of the environmental burdens at the environmental optimum with respect to GWP. FA_o stands for the feed stream containing C3 and C4, shown in the superstructure (Figs.4 and 5). FB_o stands for the feed stream containing i-C4.*

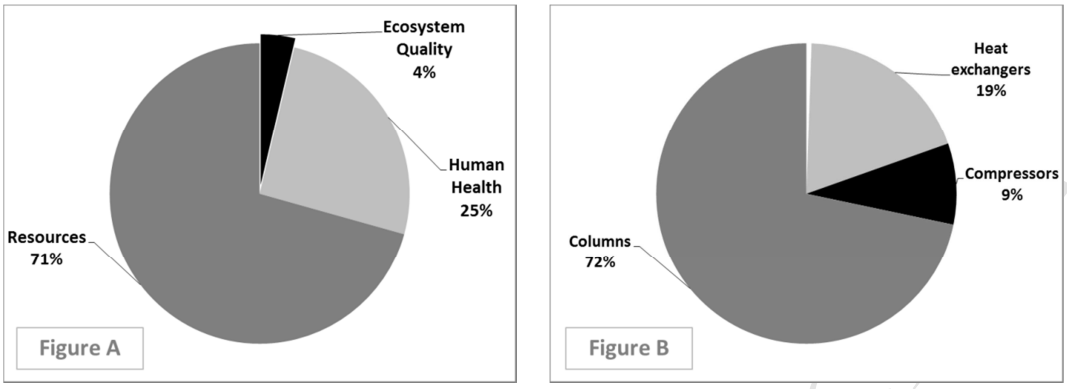

Fig. C.4. *Breakdown of the environmental burdens in terms of EI-99 at the minimum environmental impact calculated by maximizing EP and minimizing GWP.*

Highlights

A disjunctive model is used for the isobutane alkylation process

Simultaneous economic and environmental objectives are considered

New alternatives never studied before of the alkylation process are considered

A hybrid simulation-multiobjective optimization approach is used

Rigorous design is used instead of shortcuts or approximate models

Abbreviations to be placed in a footnote on the first page of the article

Life Cycle Assessment (LCA)

Multiobjective (MO)

Generalized Disjunctive Programming (GDP)

Global Warming Potential (GWP)

Ecoindicator-99 (EI-99)

Supplementary data A –

Descriptive caption: BRIEF EXPLANATION OF THE TWO ENVIRONMENTAL IMPACT METHODS CONSIDERED

EI-99 (Ecoindicator-99)

This model has three different environmental categories:

- "Human health" damages are specified in Disability Adjusted Life Years (DALYs). A damage of 1 means that 1 life year of 1 individual is lost or 1 person suffers for four years from a disability with a weight of 0.25.
- "Ecosystem quality" damages are specified as PDF × m^2× year. PDF stands for "potentially disappeared fraction" of species. A damage of 1 means that all species disappear from 1 m^2 over 1 year, or 10% of all species disappear from 1 m^2 over 10 years.
- "Resources" damages that are specified as MJ surplus energy. A damage of 1 means that due to a certain extraction of resources, further extraction of the same resources in the future will require one additional MJ of energy due to the lower concentration of resource or other unfavorable characteristics of the remaining reserves.

The parameter ($\mathrm{Eco}_{\mathrm{total}}$) for this model can be calculated for each piece of equipment according to eq. (A. 1):

$$\mathrm{Eco}_{\mathrm{total}} = \sum_{i=1}^{i=12} Eco_i \cdot Q \cdot t \qquad \text{Eq. (A.1)}$$

Where Eco_i are the different coefficients parameters taken from the Ecoinvent data set (Frischknecht et al., 2005; Hischier R., 2010) and illustrated in Table A.1; *Q* can be either the mass flow rate or the energy flow rate relative to each piece of equipment and *t* is the time that the plant needs to work to produce the functional unit.

GWP (Global Warming Potential)

GWP is one of the most widely used methods in LCA. It was developed by the Intergovernmental Panel on Climate Change (IPCC) and it is based on a characterization of different gaseous emissions according to their global warming potential of different emissions in the impact category climate change. Direct global warming potentials (GWPs) are relative to the impact of carbon dioxide. GWPs are an index for estimating the relative global warming

contribution due to atmospheric emission of a kg of a particular greenhouse gas compared to the emission of a kg of carbon dioxide. This method has three time horizons to illustrate the effects of atmospheric lifetimes of the different gases (20, 100, and 500 years). For the environmental assessment of our flow sheet, the time horizon chosen was 100 years, which is the most commonly used time horizon in these types of assessments.

Table A.1

Categories, subcategories and other basic information for the EI-99 (Frischknecht et al., 2005; Hischier R., 2010)

Categories	***Normalization***	***Average Weight***	***Subcategories***
Ecosystem Quality	0.0154 DALYs/y	40 %	Eco_1 = acidification & eutrofication Eco_2 = ecotoxicity Eco_3 = land occupation Eco_4 = stored ecotoxicity
Human Health	5130 PDF·m^2·y	40 %	Eco_5 = carcinogenics Eco_6 = climate change Eco_7 = ionizing radiation Eco_8 = ozone layer depletion Eco_9 = respiratory effects Eco_{10} = stored carcinogenics
Resources	8410 MJ/y	20 %	Eco_{11} = fossil fuel Eco_{12} = mineral extraction

The parameter (GWP) for this model can be calculated for each piece of equipment as shown in Eq. (A.2):

$$GWP = gwp \cdot Q \cdot t \qquad \text{Eq. (A.2)}$$

Where gwp is the coefficient parameter taken from the Ecoinvent data set (Frischknecht et al., 2005; Hischier R., 2010) for this model; Q can be either the mass flow rate or the energy flow

rate relative to each piece of equipment and t is the time that the plant needs to work to produce the functional unit.

Both methods, EI-99 and GWP (sections 5.2.1 and 5.2.2, respectively), are commonly used with LCA which is an objective process for evaluating the environmental loads associated with a product, process or activity. Therefore, LCA can be used as a tool for quantitative evaluation of the environmental merits or "cleanliness" of a process and for ranking process alternatives according to their cleanliness (Burgess and Brennan, 2001).

Literature

Burgess, A.A., Brennan, D.J., 2001. Application of life cycle assessment to chemical processes. Chemical Engineering Science 56, 2589-2604.
Frischknecht, R., Jungbluth, N., Althaus, H.-J., Doka, G., Dones, R., Heck, T., Hellweg, S., Hischier, R., Nemecek, T., Rebitzer, G., Spielmann, M., 2005. The ecoinvent Database: Overview and Methodological Framework (7 pp). The International Journal of Life Cycle Assessment 10, 3-9.
Hischier R., W.B., Althaus H.-J., Bauer C., Doka G., Dones R., Frischknecht R., Hellweg S., Humbert S., Jungbluth N., Köllner T., Loerincik Y., Margni M., and Nemecek T, 2010. Implementation of Life Cycle Impact Assessment Methods. Final report ecoinvent v2.2. Swiss Centre for Life Cycle Inventories, Dübendorf, CH.

Supplementary data B –

Descriptive caption: MATHEMATICAL MODEL

The problem was formulated as a hybrid simulation-optimization multi-objective generalized disjunctive programming (GDP) problem (Brunet et al., 2012; Caballero and Grossmann, 2010; Caballero et al., 2005) and solved using our implementation of the logic based outer approximation algorithm (Türkay and Grossmann, 1996) .

Conceptually the model can be written as follows:

$$\min : \left\{ f_{Ec}(\mathbf{x_D}, \mathbf{x_I}), f_{En}(\mathbf{x_D}, \mathbf{x_I}) \right\} \qquad \text{Eq. (B.1)}$$

$$s.t. \quad \mathbf{x_D} = \mathbf{r}_{im}(\mathbf{x_I}) \qquad \text{Eq. (B.2)}$$

$$\mathbf{r}_{ex}(\mathbf{x_D}, \mathbf{x_I}) = \mathbf{0} \qquad \text{Eq. (B.3)}$$

$$\mathbf{s}_{ex}(\mathbf{x_D}, \mathbf{x_I}) \leq \mathbf{0} \qquad \text{Eq. (B.4)}$$

$$\begin{bmatrix} Y_i \\ \mathbf{x_D} = \mathbf{h}_{im,i}(\mathbf{x_{I,}}_i) \\ \mathbf{h}_{ex,i}(\mathbf{x_D}, \mathbf{x_{I,}}_i) = \mathbf{0} \\ \mathbf{g}_{ex,i}(\mathbf{x_D}, \mathbf{x_{I,}}_i) \leq \mathbf{0} \end{bmatrix} \veebar \begin{bmatrix} \neg Y_i \\ \mathbf{x_{I,}}_i = \mathbf{0} \end{bmatrix} \quad \forall\, i \in D \qquad \text{Eq. (B.5)}$$

$$\Omega\left(\mathbf{Y}\right) = True \qquad \text{Eq. (B.6)}$$

$$\mathbf{x_I} \in X \subseteq \Re^n \qquad \text{Eq. (B.7)}$$

$$\mathbf{Y} \in \left\{ True,\ False \right\}^p \qquad \text{Eq. (B.8)}$$

where f_{Ec} and f_{En} are the economic and the environmental objective functions respectively. $\mathbf{x_D}$ is a vector of dependent variables (e.g calculated by the process simulator Aspen-HYSYS™) over which the designer has no direct control. $\mathbf{x_I}$ is a vector of independent variables over which the user has complete control. The index "*im*" makes reference to *implicit* equations calculated by third party models (Process Simulator, other Matlab models, etc.) and the index "*ex*" makes reference to explicit equations. Note that we have introduced dependent variables in explicit equations (for example in $\mathbf{r}_{ex}(\mathbf{x_D}, \mathbf{x_I}) = \mathbf{0}$ or $\mathbf{s}_{ex}(\mathbf{x_D}, \mathbf{x_I}) \leq \mathbf{0}$). Implicitly, this formulation involves sequential function evaluation, first the implicit models and then the

explicit equations. The Boolean variables Y_i will take the value 'True' if equipment 'i' is selected and 'False' otherwise, where “p” is the number of Boolean variables.

The disjunctions shown in Eq. (B.5) explicitly state that if a given piece of equipment is selected then all the equations related to it must hold, otherwise all the independent variables related to that piece of equipment are set to zero and the dependent variables calculated for that piece of equipment are simply ignored. In the model given by Eq. (B.5) we only allow two term disjunctions which is the case of process networks and synthesis problems, applicable in this work.

The only fixed equipment (i.e., they are present in all the alternative configurations) are the initial feed compressors, the settling tank, the reactants recycle pump and the C8 distillation column that necessarily will appear at the end of any separation configuration. The reason for this is that this separation is performed at lower pressure (1 bar) than the other separations (8 bar). The remaining distillation columns must be included inside a disjunction.
All the thermodynamic properties and all the equipment simulations, apart from the distillation columns, are calculated by the process simulator Aspen-HYSYS ™. For the distillation column simulations we use the shortcut method by Underwood (1948), Fenske (1932), Gilliland (1940) with the explicit equation by Molokanov et al. (1972) and Kirkbride (1944) for the feed tray location implemented in Matlab ™ and connected to Aspen HYSYS through the activeX capabilities (in any case, the final results were checked with a rigorous model). Physical properties (e.g. estimation of relative volatilities) and condensers and reboilers were rigorously calculated using Aspen-HYSYS. For the simulation of thermal couples we follow the approach introduced by Navarro-Amorós et al. (2013) The details of the calculation of sequence of distillation columns are too bulky to be included here. However, a comprehensive description can be found in references Caballero and Grossmann (2001, 2006, 2013). We would at least like to remark that all the alternatives from conventional to fully thermally coupled configurations (including divided wall columns) have been included.
In order to get feasible configurations a set of logical relationships must be included, represented in Eq. (B.6) as $\Omega\left(\mathbf{Y}\right) = True$. The Boolean variables and the logical relationships used in this work are the following:

Y_{Reator}^{Iso}	The isothermal reactor is selected.
Y_{Reator}^{Auto}	The auto-refrigerated reactor is selected. Inside this disjunction, apart from the reactors, it includes the compressor (K3), cooler (HX1) and recycle pump (see Fig.3).
Y_{C_3/C_4}^{Pre}	Feed pre-fractionator for separating C3 from C4. (Components heavier than C4 are included in bottoms)
$Y_{C_3/C_4C_8...}$	Separation of C3 from C4 and heavier components in the main separation block.
$Y_{C_3C_4/C_8...}$	Separation of C4 from C8 in the main separation block.
Y_{C_3/C_4}	Separation of C3 from C4. There are no heavier components than C4 in the feed stream.
Y_{C_4/C_8}	Separation of C4 from C8. There are no lighter components than C4 in the feed stream.
$Y_{C_3/C_4C_8...}^{b}$	Separation of C3 from C4 performed in parallel with C4/C8.
$Y_{C_3C_4/C_8...}^{b}$	Separation of C4 from C8 performed in parallel with C3/C4.
$Y_{C_3C_4/C_4C_8}$	Separation of C3 from C8, the intermediate volatility components (C4) are allowed to optimally distribute themselves between distillate and bottoms (These are the cases of pre-fractionator and divided wall column)
Y_{DWC}	The divided wall column is included.
$H_{C_3C_4}$	There is a condenser in the mixture C3C4.
$H_{C_4C_8...}$	There is a reboiler in the mixture C4C8 and heaviest C12.
$H_{C_4}^{Reb}$	There is a reboiler in stream C4.
$H_{C_4}^{Cond}$	There is a condenser in stream C4.

- The isothermal reactor or the autorefrigerated reactor must be selected:

$$Y_{Reator}^{Iso} \veebar Y_{Reator}^{Auto} \qquad \text{Eq. (B.9)}$$

- If the feed stream pre-fractionator (C3/C4) is selected, then the C3/C4 separation in the rest of the superstructure must not be selected:

$$Y_{C_3/C_4}^{Pre} \Rightarrow \left(\neg Y_{C_3/C_4C_8} \wedge \neg Y_{C_3/C_4C_8}^{b} \right) \qquad \text{Eq. (B.10)}$$

Note that these constraints could eventually be removed. It is not possible to perform a complete (100%) separation of C3 from C4; therefore as a result of the recycle there

occurs C3 accumulation in the process. A small purge is then needed. There is a tradeoff between the reduced flow due to preceding separation and the purge losses, which must be optimized. If the accumulation is too large a new C3/C4 splitter would be needed, but maybe in this case having the C3/C4 pre-fractionator makes no sense.

- At most one of the initial separations in the main separation block must be selected:

$$at\ most(Y_{C_3/C_4C_8};Y_{C_3C_4/C_8};Y_{C_3C_4/C_4C_8}) \quad \text{Eq. (B.11)}$$

- Connectivity relations:

$$Y_{C_3/C_4C_8} \Rightarrow Y_{C_4/C_8} \quad \text{Eq. (B.12)}$$

$$Y_{C_3C_4/C_8} \Rightarrow Y_{C_3/C_4} \quad \text{Eq. (B.13)}$$

$$Y_{C_3C_4/C_4C_8} \Rightarrow Y_{C_3/C_4} \wedge Y_{C_4/C_8} \quad \text{Eq. (B.14)}$$

$$Y_{DWC} \Rightarrow Y_{C_3C_4/C_4C_8} \wedge Y_{C_3/C_4} \wedge Y_{C_4/C_8} \quad \text{Eq. (B.15)}$$

$$Y_{C_3/C_4} \Rightarrow Y_{C_3C_4/C_8} \vee Y_{C_3C_4/C_4C_8} \quad \text{Eq. (B.16)}$$

$$Y_{C_4/C_8} \Rightarrow Y_{C_3/C_4C_8} \vee Y_{C_3C_4/C_4C_8} \quad \text{Eq. (B.17)}$$

- Relationships between columns and heat exchangers. (Explicit consideration of thermal couples)

$$H_{C_3C_4} \Rightarrow Y_{C_3C_4/C_8} \vee Y_{C_3C_4/C_4C_8} \quad \text{Eq. (B.18)}$$

$$H_{C_4C_8} \Rightarrow Y_{C_3/C_4C_8} \vee Y_{C_3C_4/C_4C_8} \quad \text{Eq. (B.19)}$$

$$H_{C_4}^{Reb} \Rightarrow Y_{C_3/C_4} \wedge \neg Y_{C_4/C_8} \quad \text{Eq. (B.20)}$$

$$H_{C_4}^{Cond} \Rightarrow \neg Y_{C_3/C_4} \wedge Y_{C_4/C_8} \quad \text{Eq. (B.21)}$$

$$Y_{DWC} \Rightarrow \neg H_{C_3C_4} \wedge \neg H_{C_4C_8} \wedge \neg H_{C_4}^{Reb} \wedge \neg H_{C_4}^{Cond} \quad \text{Eq. (B.22)}$$

Note that if a heat exchanger does not exist then the flow transfer between two columns is performed by a thermal couple.

The sizing, costing and environmental impact of every one of the variable equipment is included inside its disjunction. In this way, these equations are only included if the equipment is selected.

It is also worth remarking that all the flowsheet alternatives have a recycle stream. It is possible to allow the process simulator to converge the recycle however, it is much more

efficient to let the optimizer converge it, for two reasons: First, if the process simulator converges the recycle it is equivalent to performing a complex iterative calculation each time the optimizer calls the flow sheet in the process simulator, including a derivative calculation which is very time consuming. And second, the flowsheet calculation in the process simulation is slightly noisy – small numerical errors are introduced each time that a unit operation is solved – and recycles behave as noise amplifiers which can eventually produce an unexpected behavior of the optimizer. Therefore it is best to let the optimizer converge the recycle. This implies explicitly including a new set of independent variables and the equivalent set of constraints.

To solve the MO optimization problem we use the epsilon constraint method (Ehrgott, 2005). For this we need to first find the two extremes of the Pareto curve (Fig. 1), i.e., we need to solve a single-objective optimization problem for each one of the objectives: optimization of the economic potential and the environmental objective. Once we have determined the two extremes of the Pareto curve, then we have to reformulate the problem in Eqs. (B.1) to (B.8) and move all but one of the objectives to the constraints. For the present research, we decided to move the environmental objective to the constraints.

$$\min : f_{Ec}(\mathbf{x_D}, \mathbf{x_I}) \qquad \text{Eq. (B.23)}$$

$$s.t. \quad f_{En}(\mathbf{x_D}, \mathbf{x_I}) \leq \varepsilon \qquad \text{Eq. (B.24)}$$
$$rest\ of\ model\ in\ (1 to 8)$$

Finally, we solve a sequence of single-objective problems in which the epsilon (ε) value is changed between the two extreme values of the environmental indicator in the Pareto curve under construction.

Due to model complexity, it is convenient to focus only on the variables that affect most of the system. Therefore a sensitivity analysis was performed beforehand and the following continuous variables were finally considered for the present study:

a. The molar flowrate ratio of the two fresh input streams ($F_{i\text{-}C4}/F_{C3+C4}$).
b. The volume of the reactor(s).
c. The temperature of the refrigerated reactor.
d. The split fraction in the purge stream.
e. Individual flows and temperature in the recycle stream.

Preliminary studies showed that the temperature in the reactor was always optimized to the lowest value in the given range since the main reaction has a lower activation energy as compared to the secondary reaction and also because at higher temperatures polymerization of the olefins becomes significant and the yield decreases (Gary and Handwerk, 2001). Therefore, a fixed value was chosen. This temperature value should not be very low since the acid viscosity could increase to such a value that good mixing of the reactants becomes difficult (Gary & Handwerk, 2001). Finally, its value was fixed at – 5 ºC following the temperature value used in Dimian and Bildea (2008).

In the distillation columns, the recovery of key components was fixed at 0.99. A sensitivity analysis, always assuming a sharp separation, showed that using other values has no major impact on the results.

The reflux ratio was fixed at 1.3 times the minimum. This last assumption is just a rule of thumb applicable to distillation columns; some simulations showed that this value is always near the optimal solution. In any case, its value does not change the optimal solution and as we are comparing alternatives the only effect could be to slightly shift the Pareto curve without any qualitative modification in the results.

It is worth noting that the model we are dealing with is non-convex. Under such conditions, gradient based algorithms can ensure only a local minimum. In this particular case, however, the fact that the same optimal solution was reached from different starting points and the smooth shape of the Pareto curve seem to indicate that the solution is likely to be the global optimal solution.

Literature

Brunet, R., Cortés, D., Guillén-Gosálbez, G., Jiménez, L., Boer, D., 2012. Minimization of the LCA impact of thermodynamic cycles using a combined simulation-optimization approach. Appl. Therm. Eng. 48, 367-377.

Caballero, J.A., Grossmann, I.E., 2001. Generalized Disjunctive Programming Model for the Optimal Synthesis of Thermally Linked Distillation Columns. Ind. Eng. Chem. Res. 40, 2260-2274.

Caballero, J.A., Grossmann, I.E., 2006. Structural Considerations and Modeling in the Synthesis of Heat-Integrated−Thermally Coupled Distillation Sequences. Ind. Eng. Chem. Res. 45, 8454-8474.

Caballero, J.A., Grossmann, I.E., 2010. Hybrid Simulation-Optimization Algorithms for Distillation Design, in: Pierucci, S., Ferraris, G.B. (Eds.), Computer Aided Chemical Engineering. Elsevier, pp. 637-642.

Caballero, J.A., Grossmann, I.E., 2013. Synthesis of complex thermally coupled distillation systems including divided wall columns. AIChE J. 59, 1139-1159.

Caballero, J.A., Milán-Yañez, D., Grossmann, I.E., 2005. Rigorous Design of Distillation Columns: Integration of Disjunctive Programming and Process Simulators. Ind. Eng. Chem. Res. 44, 6760-6775.

Dimian, A.C., Bildea, C.S., 2008. Chemical process design : computer-aided case studies. Wiley-VCH, Weinheim Chichester.

Ehrgott, M., 2005. Multicriteria optimization, 2nd ed. Springer, Berlin ; New York.

Fenske, M.R., 1932. Fractionation of Straight-Run Pennsylvania Gasoline. Ind. Eng. Chem. 24, 482-485.

Gary, J.H., Handwerk, G.E., 2001. Petroleum refining : technology and economics, 4th ed. Marcel Dekker, New York.

Gilliland, E.R., 1940. Multicomponent Rectification Estimation of the Number of Theoretical Plates as a Function of the Reflux Ratio. Ind. Eng. Chem. 32, 1220-1223.

Kirkbride, C.G., 1944. Process design procedure for multicomponent fractionators. . Petroleum Refiner. 23, 321-336.

Molokanov, Y.K., Korablina, T.P., Mazurina, N.I., Nikiforov, G.A., 1972. An Approximation Method for Calculating the Basic Parameters of Multicomponent Fraction. Int. Chem. Eng. 12, 209.

Navarro-Amorós, M.A., Caballero, J.A., Ruiz-Femenia, R., Grossmann, I.E., 2013. An alternative disjunctive optimization model for heat integration with variable temperatures. Comput. Chem. Eng. 56, 12-26.

Türkay, M., Grossmann, I.E., 1996. Logic-based MINLP algorithms for the optimal synthesis of process networks. Comput. Chem. Eng. 20, 959-978.

Underwood, A., 1948. Fractional distillation of multicomponent mixtures. Chemical Engineering Progress 44, 603-614.

Supplementary data C –

Descriptive caption: DETAILED ANALYSIS OF ALL OF THE RESULTS OBTAINED

According to the calculations explained in the main body of the manuscript, the functions EP, GWP and EI-99 are evaluated at every iteration during the optimization process. The optimization is accomplished by maximizing EP and minimizing either one of the two environmental indicators selected beforehand. But even though the optimization was conducted by selecting only one of the two environmental indicators at a time, we have also included the readings of the other environmental indicator in the final results. Hence, the optimized solution consists of one EP value and the optimized value of the preselected environmental indicator, and also includes a reading for the other environmental indicator under the optimized conditions. The total amount of information captured during the optimization process is considerable when this approach is taken. In addition, we have calculated and recorded a breakdown of all of the environmental burdens. We summarize and present all this information as a collection of charts.

As stated previously, the two Pareto curves are rather similar, so it would be enough to analyze the detailed results of just one of them. To that end, we present a thorough analysis of the breakdown of the environmental impacts when the system is optimized in terms of the GWP environmental indicator. Nonetheless, they will be discussed in terms of both indicators – the optimized GWP results as well as the corresponding EI-99 readings.

Fig. C.1 and C.2 display information regarding the economic optimum corresponding to point A in Fig.6 (main body). Figs. C.3 and C.4 provide details about the environmental optimum, point B in Fig.6. In Fig. C.1, a breakdown of the environmental impacts for the solution that is optimal with respect to EP and GWP is presented. Fig. C.1.A contains the optimized GWP

results and Fig. C.1.B includes a breakdown of the EI-99 results calculated from the optimized configuration based on GWP.

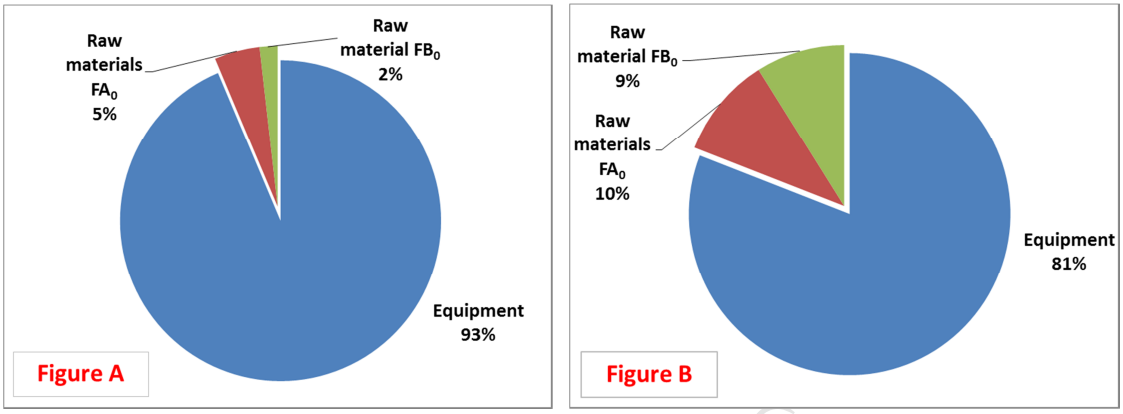

Fig. C.1. *Breakdown of the environmental impacts at optimum economic potential when the system is optimized using GWP as the environmental indicator. Figure A and Figure B show GWP and EI-99 readings respectively.FA_o stands for the feed stream containing C3 and C4, shown in the superstructure (Fig.4). FB_o stands for the feed stream containing i-C4*

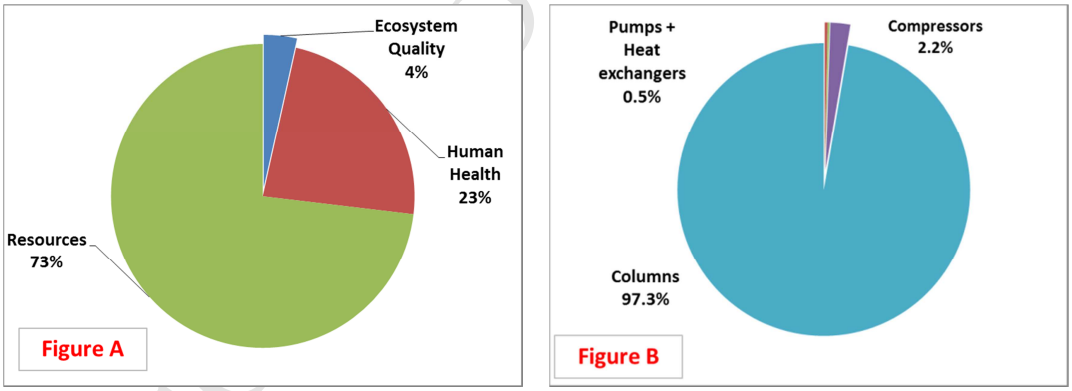

Fig C.2. *Breakdown of the environmental burdens at optimum economic potential according to Ecoindicator-99, when the superstructure is optimized using EP and GWP (Point A on the GWP Pareto curve in Fig. 6).*

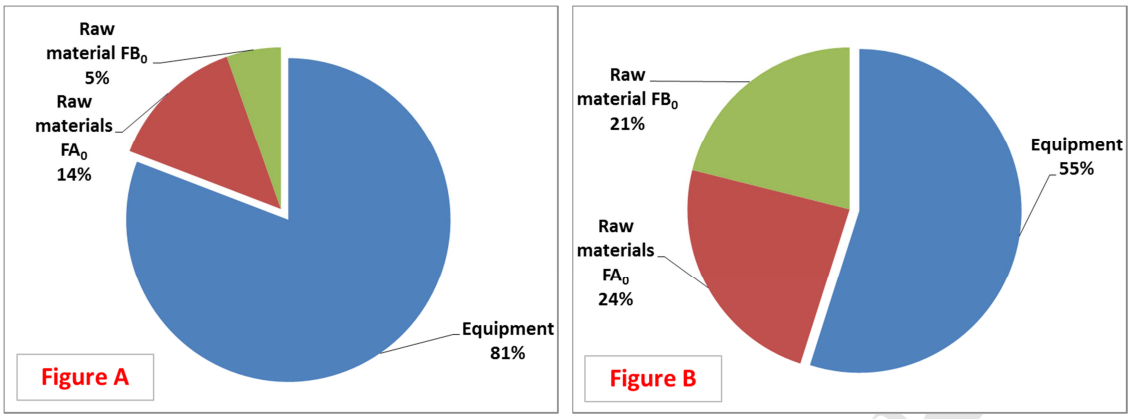

Fig. C.3. *Breakdown of the environmental burdens at the environmental optimum with respect to GWP. Figure A and Figure B show GWP and EI-99 readings respectively. FA_o stands for the feed stream containing C3 and C4, shown in the superstructure (Figs.4 and 5). FB_o stands for the feed stream containing i-C4.*

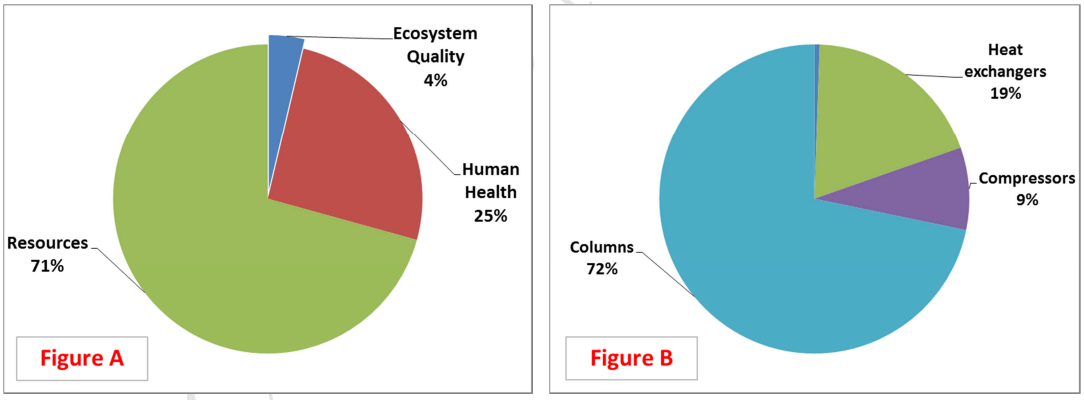

Fig. C.4. *Breakdown of the environmental burdens in terms of EI-99 at the minimum environmental impact calculated by maximizing EP and minimizing GWP.*

Since most of the environmental burden due to a process can be ascribed to the equipment operation, it seems reasonable to conduct a thorough analysis of the role of the latter in terms of the categories in EI-99 (supplementary data). The results of such an analysis are shown in

Fig. C.2, where it is possible to identify the distribution of the 81% corresponding to equipment in Fig. C.1.A over the type of environmental damage (Fig. C.2.A) and the type of equipment (Fig. C.2.B) at the economic optimum with respect to GWP. As expected, the type of environmental damage referred to as 'Resources' contributes the most (73%) to the EI-99 total value due to the 'fossil fuels' impact subcategory.

Fig. C.2.B shows that the greatest contribution to environmental burden comes from the energy required to operate all the columns (Column3, Column4 and Column8) shown in the 3rd solution. This figure also illustrates that the reactors have no impact at all since they are auto-refrigerated. Therefore, when the superstructure is optimized only with respect to the economic criterion, the system tries to reduce the variable costs associated with the operation of the distillation columns (boilers and condensers).

Repeating a similar analysis for the other extreme of the Pareto curve, which represents the locus of the environmental optimum (point B on the GWP Pareto curve in Fig. 6), we find some differences with respect to the economic optimum shown in Figs. C.3 and C.4.

Fig. C.3 again demonstrates that the equipment contributes the most to the environmental burden. Fig. C.3.A shows that the optimization is mainly accomplished by minimizing energy consumption (in equipment), which is the main source of CO_2 emission into the atmosphere. The EI-99 readings (Fig. C.3.B) carried out alongside the optimization exhibits a reduction in the impacts associated with the equipment (due mainly to the reduced energy requirements when a divided wall column is used). This implies an increase in relative weight of the raw materials based on the way their toxicity is factored into the EI-99 value.

We obtain Fig. C.4 by the same procedure that led to Fig. C.2, but from the environmental optimum on the GWP Pareto curve. In Fig. C.4.A the category “Resources” demonstrates yet again that the highest environmental impact occurs in the form of the energy consumption. This is the most important factor affecting the superstructure under study and is accounted for in the impact subcategory named “Fossil fuels”. Fig. C.4.B exhibits similar results to Fig. C.2.B, although now the environmental impact is also associated with the heat exchanger used to refrigerate the reactor.